DOI: 10.1002/asia.200800122

Penta(pyrenyl)[60]fullerenes: Pyrene–Pyrene and [60]Fullerene–Pyrene Interactions in the Crystal and in Solution

Yutaka Matsuo,*[a] Kouhei Morita,[b] and Eiichi Nakamura*[a, b]

Dedicated to Professor Ryoji Noyori on the occasion of his 70th birthday

Abstract: A new type of fullerene–pyrene hybrid molecule, $C_{60}Ar_5R$ [Ar = 1-pyrenyl, 4-(1-pyrenyl)C_6H_4, 4-{(1-pyrenyl)CO_2}C_6H_4, and 4-{(1-pyrenyl)-$(CH_2)_3CO_2$}C_6H_4; R = H and Me] was synthesized by a regioselective penta-addition reaction using organocopper reagents. The compounds were investigated using electrochemical measurements, DFT calculations, single-crystal X-ray structural analysis, and spectroscopic and fluorescence measurements. Intramolecular and intermolecular fullerene–pyrene and pyrene–pyrene interactions were characterized in the crystals. Fluorescence measurements in dilute solutions suggested the presence of intramolecular fullerene–pyrene and pyrene–pyrene interactions.

Keywords: energy transfer · fluorescence spectroscopy · fullerene · pi interactions · pyrene

Introduction

Fullerene derivatives bearing light-absorbing fragments,[1] and their supramolecular assembly,[2] have been the subject of numerous studies related to interest in photovoltaic devices and in light-harvesting systems in nature.[3] Among them, covalently multifunctionalized molecules bearing several integrated chromophores on the fullerene core have attracted special attention.[4,5] Such multifunctionalized molecules are, however, almost inevitably very large, and consequently, their synthesis requires many synthetic steps. Herein, we report on a quick and effective synthesis of [60]fullerene derivatives that bear five pyrene units, on the structural analysis of these molecules and their molecular assembly in crystals, and on their absorption and emission spectra. From these data, we can elucidate the structural dependence of the energy transfer between the excited state of the pyrene moieties and the fullerene core.

[a] Dr. Y. Matsuo, Prof. E. Nakamura
Nakamura Functional Carbon Cluster Project
ERATO Japan Science and Technology Agency (JST)
Hongo, Bunkyo-ku, Tokyo 113-0033 (Japan)
Fax: (+81) 3-5841-1476; (+81) 3-5800-6889
E-mail: matsuo@chem.s.u-tokyo.ac.jp
nakamura@chem.s.u-tokyo.ac.jp

[b] K. Morita, Prof. E. Nakamura
Department of Chemistry
The University of Tokyo
Hongo, Bunkyo-ku, Tokyo 113-0033 (Japan)

Supporting information for this article is available on the WWW under http://dx.doi.org/10.1002/asia.200800122.

Results and Discussion

Synthesis of the Penta(pyrenyl)[60]fullerene Derivatives

In this paper, we describe the synthesis of four penta(pyrenyl)[60]fullerene derivatives that have five pyrenyl groups with either a direct connection or phenylene, phenylene-oxycarbonyl, and phenylene-oxycarbonylpropyl spacers (Scheme 1). Compounds **1** and **2** were prepared in a single step, and compounds **3** and **4** in several steps. The regioselective penta-arylation reaction of 1-pyrenyl and 4-(1-pyrenyl)phenyl Grignard reagents[6] with [60]fullerene in the presence of a copper salt afforded **1** and **2** in a near-quantitative yield. The reaction required moderate heating (40 °C), which perhaps indicates that these hindered Grignard reagents are less reactive than the corresponding phenyl reagent. To obtain **3** and **4**, we first synthesized penta(4-hydroxyphenyl)[60]fullerene[7] from the reaction of [60]fullerene with a [4-(tetrahydropyranyloxy)phenyl]copper reagent, followed by deprotection of the tetrahydopyranyl group with a catalytic amount of *p*-toluenesulfonic acid. Esterification of the penta(hydroxyphenyl)[60]fullerene with pyrenecarboxylic and 3-(1-pyrenyl)propanoic acid chlorides in the presence of a base produced the expected pentapyrenyl compounds **3** and **4**. All the pyrenyl compounds were ob-

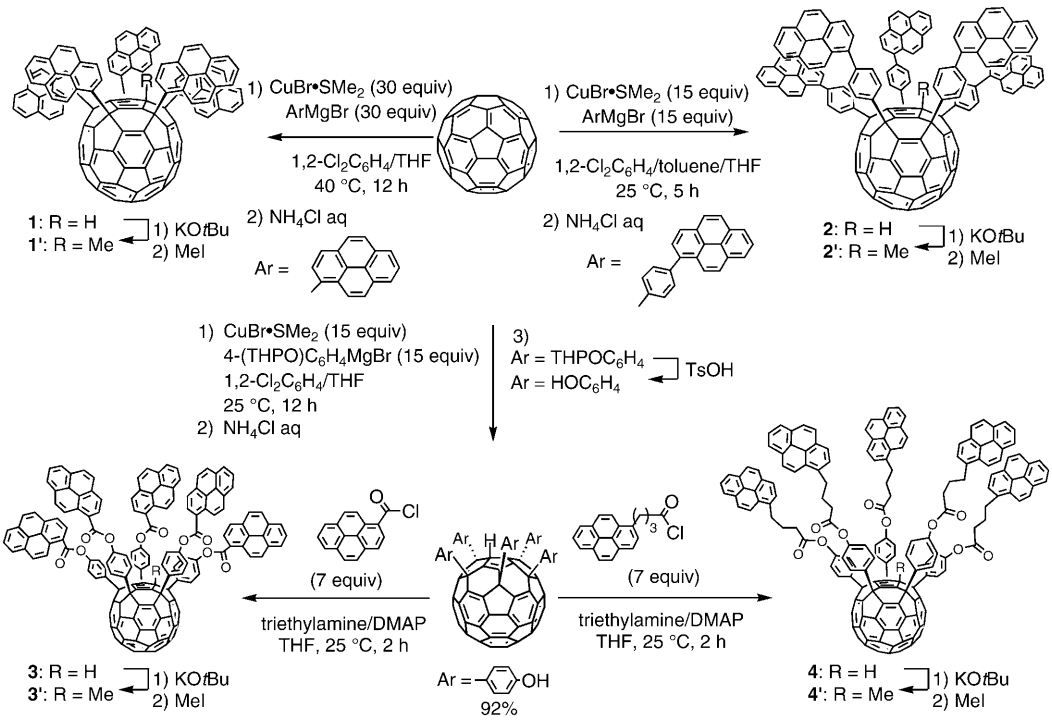

Scheme 1. Synthesis of penta(pyrenyl)[60]fullerenes. THP = tetrahydopyranyl, DMAP = 4-dimethylaminopyridine.

tained in moderate to good overall yields, and were acceptably stable in air. Compound **1** showed poor solubility in all solvents, but compounds **2**–**4** were much more soluble, for example, in aromatic solvents, CS_2, THF, chloroform, and dichloromethane. In particular, compound **4** showed good solubility, even in aliphatic solvents. Characterization of the compounds was performed using NMR and MS, as well as X-ray crystallography for **1** and **3**.

We also synthesized the corresponding methylated compounds, C_{60}(1-pyrenyl)$_5$Me (**1′**), $C_{60}[C_6H_4$-(1-pyrenyl)$]_5$Me (**2′**), $C_{60}[C_6H_4$-OCO-(1-pyrenyl)$]_5$Me (**3′**), and $C_{60}[C_6H_4$-OCO-$(CH_2)_3$-(1-pyrenyl)$]_5$Me (**4′**), which were obtained by deprotonation of **1**–**4** and subsequent electrophilic methylation with methyl iodide in quantitative yield.[8] In contrast to **1** to **4**, which tended to be oxidized on standing and were reactive under reducing electrochemical conditions,[9] the methylated products were very stable in solution under air for a long period. Therefore, the methylated products were used in the electrochemical experiments, while the protio compounds were used for crystallographic and spectroscopic analyses.

The ^{1}H NMR spectra of these compounds are of interest (Figure 1). First, the C_1-symmetric pattern of the spectrum of **1′** (Figure 1, bottom), owing to a restriction on the rotation of the pyrene groups, was apparent. This is in contrast to the C_s-symmetric pattern of **1** (Figure 1, top) and the other flexible compounds, **2**–**4** and **2′**-**4′** (data not shown). The magnetic anisotropic effects of the fullerene π-electron-conjugated system caused the protons at the C1″ and C9 positions in **1** and **1′** to undergo large changes in their chemical shift. Thus, the signals owing to the C9 pyrene protons in **1** and **1′** (e.g., $\delta = 9.87$ ppm in **1**) are shifted significantly downfield in comparison to pyrene itself ($\delta = 8.1$ ppm). In contrast, the C1″ pyrene protons were shifted significantly upfield (e.g., $\delta = 5.30$ ppm in **1** vs. 7.66 ppm for pyrene).

Electrochemical Properties and Electronic Structures of the Penta(pyrenyl)[60]fullerene Derivatives

Cyclic voltammetric analysis of the pentapyrenylated derivatives was performed to investigate the electronic perturbation of the fullerene unit by the five pyrene groups. Compounds **1′**–**4′** exhibited two reversible one-electron reductions for the fullerene part, and one reversible three- to five-electron reduction for the five pyrene groups (Figure 2). The first and second reduction potentials (−1.31 and −1.81 V, respectively, versus a ferrocene/ferrocenium couple) owing to the fullerene 50π-electron system were shifted to the positive side compared to the reference pentaaryl compound, $C_{60}(C_6H_4$-*n*Bu-4$)_5$Me (Figure 3), because of

Abstract in Japanese:

[60]フラーレンに５つのピレニル基が結合し，異なる長さのスペーサーをもつ４種類の五重付加型[60]フラーレン誘導体を合成した．X線構造解析，電気化学測定，DFT計算，各種スペクトル測定により，分子間および分子内におけるフラーレン-ピレン間およびピレン-ピレン間の相互作用を調べた．結晶中，スペーサーの長さに応じて，分子が縦軸方向にスタックしてできるカラム状構造や，横軸方向に分子が密接する構造をとることを明らかにした．また，溶液中での蛍光スペクトル測定において，全ての分子においてピレン部位からフラーレン部位へのエネルギー移動が観測され，スペーサーの長さによっては分子内ピレン-ピレン相互作用がみられた．

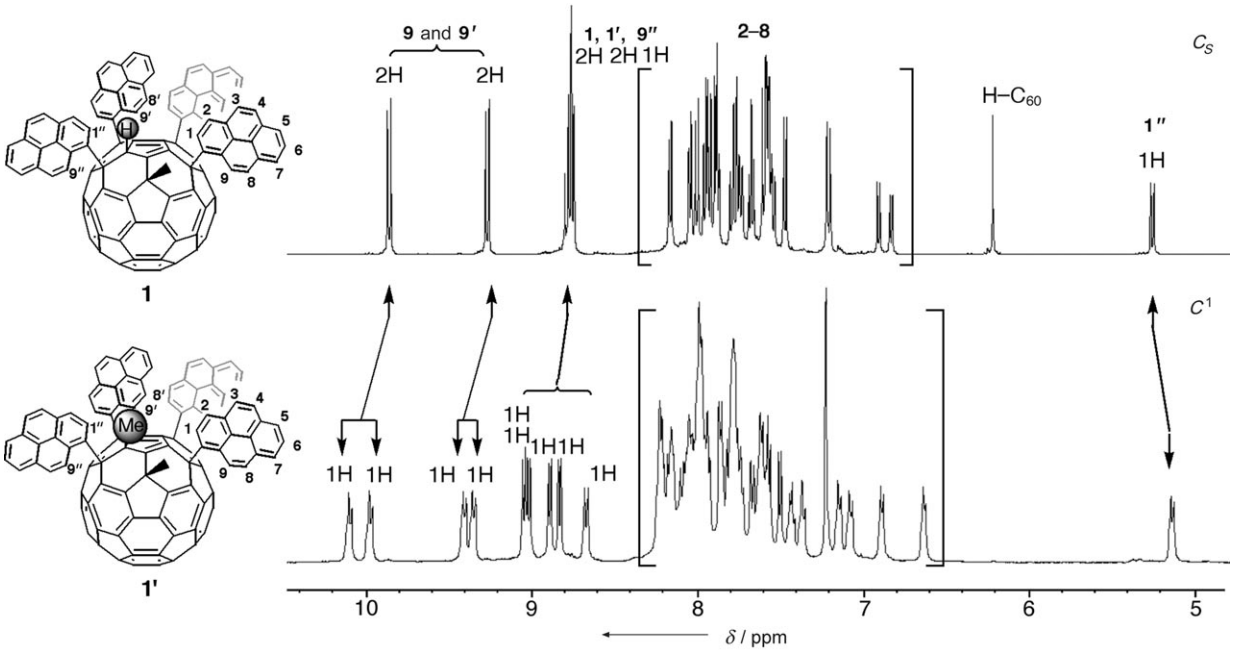

Figure 1. ^{1}H NMR spectra of the penta(pyrenyl)[60]fullerenes **1** and **1′** in $CDCl_3$ at 25 °C.

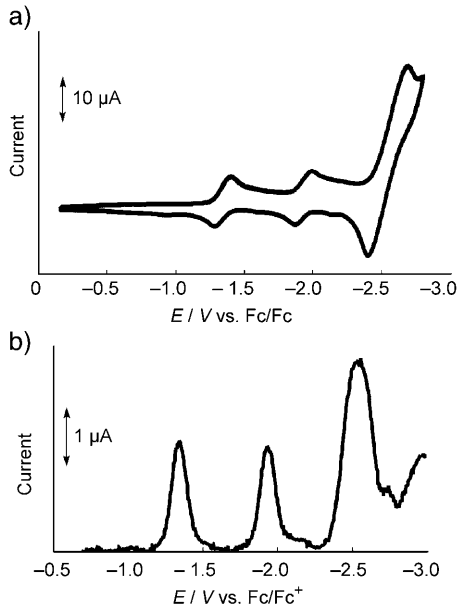

Figure 2. Electrochemical propeties of **2′**. a) Cyclic voltammogram. b) Differential pulse voltammogram. Both measurements were performed at 25 °C in a THF solution containing nBu$_4$NClO$_4$ as a supporting electrolyte.

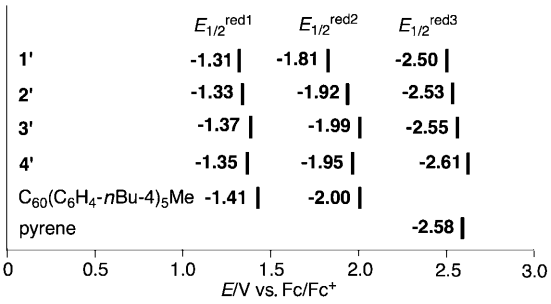

Figure 3. Reduction potentials of the penta(pyrenyl)[60]fullerenes **1′**–**4′**, reference compound, and pyrene at 25 °C in a THF solution containing nBu$_4$NClO$_4$ as a supporting electrolyte.

the electron-withdrawing nature of the pyrene unit. This tendency was observed most conspicuously in **1′**, where the pyrene unit is directly connected to the fullerene core.

DFT calculations of **1** at the B3LYP/6-31G* level were performed to study the molecular orbital characteristics. The lowest unoccupied molecular orbital (LUMO = −2.857 eV) is localized at the fullerene 50π-electron system (Figure 4a), while the lowest unoccupied molecular orbital of the pyrene part was observed at −1.769 eV as LUMO+4 (see the Supporting Information). The highest occupied molecular orbital (HOMO) is localized on the pyrene groups (Figure 4b). We can surmise that the HOMO–LUMO orbital interaction between the pyrene part and the fullerene core may have a favorable effect on the formation of the one-dimensional head-to-tail stacking of the molecules, as discussed later.

X-ray Structural Analysis and Supramolecular Interactions in the Crystals

X-ray crystallographic analysis of **1** and **3** revealed two different types of intermolecular interactions in the crystals (Figures 5–8). Single crystals suitable for X-ray diffraction analysis were obtained by slow diffusion of ethanol into a solution of **1** in CS_2 and a solution of **3** in chloroform.

CHEMISTRY
AN ASIAN JOURNAL

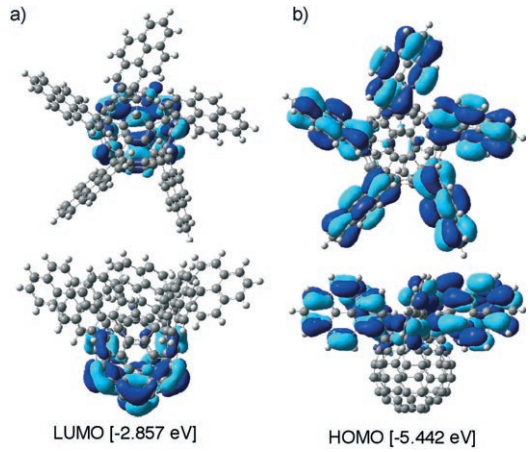

Figure 4. Molecular orbital representation of **1**: a) LUMO; b) HOMO. The data were obtained from DFT calculations (B3LYP/6-31G*).

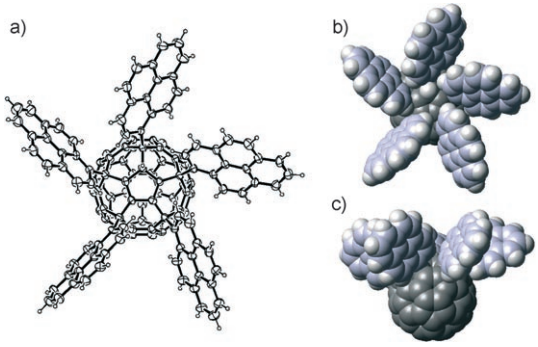

Figure 5. The molecular structure of **1**. a) ORTEP drawing with thermal ellipsoids at the 30% probability level. Solvent molecules have been omitted for clarity. b) A top view of the CPK model. c) A side view of the CPK model.

In the crystal structure of **1**, the pyrene groups form a propeller-like arrangement from the steric repulsion between the hydrogen atom on the fullerene skeleton and the hydrogen atom of the neighboring pyrene group (Figure 5b). The picture in Figure 5b combined with molecular modeling suggests that a slight twisting of the two neighboring pyrene units allows them to assume a near-parallel orientation that is suitable for photoexcimer formation in solution (see below).

The distance between the two fullerene molecules of **1** in a unit cell is 10.2 Å (compare the van der Waals distance between [60]fullerene molecules in their face-centered cubic crystal of 10.0 Å), and hence, the fullerene π surfaces are pushed tightly against each other. In addition, it can be seen that the fullerene π and the pyrene π surfaces interact with each other (Figure 6b). This interaction holds the two molecules together side by side, as seen in Figure 6a and b. We can surmise that the 1-pyrene unit is too small to embrace the second molecules of **1** to form the linear array observed in **3**.

The crystal structure of **3** showed an entirely different supramolecular profile, because of the deep, cup-shaped

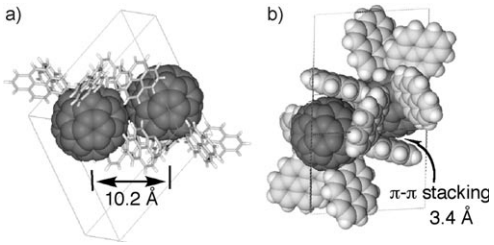

Figure 6. Crystal packing of **1**. a) A side view. b) A view displaying the π–π stacking between the fullerene and the pyrene groups. The crystal is triclinic, space group $P\bar{1}$, $a=16.883(5)$ Å, $b=17.771(5)$ Å, $c=18.157(5)$ Å, $\alpha=107.007(5)°$, $\beta=103.635(5)°$, $\gamma=103.635(5)°$, $V=4456.0(2)$ Å^3.

cavity[10] formed by the phenylene-oxycarbonyl spacer (Figure 7). We can readily see that the fullerene moiety in **3** is surrounded by the pyrene units of the next nearest neighbor (Figure 8a), and therefore forms a one-dimensional columnar array. The fullerene moiety cannot have a direct interaction with the fullerene moiety of the neighboring molecules (unlike in **1**, as shown in Figure 6a), but instead, the pyrene groups interact with the pyrene groups of the nearest neighbor (Figure 8a) to form a quasi-hexagonal packing with an antiparallel arrangement (Figure 8b). The fullerene–

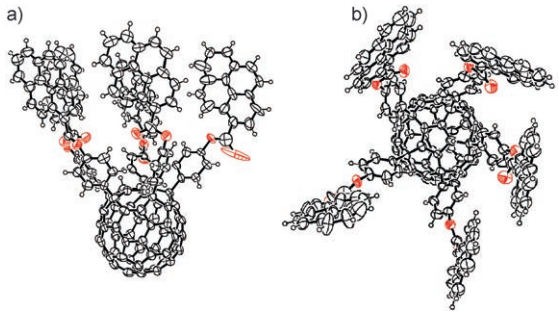

Figure 7. ORTEP drawing of **3** with thermal ellipsoids at the 30% probability level. a) A side view. b) A top view. Crystals suitable for X-ray analysis were obtained as **3**·4 $CHCl_3$. The solvent molecules have been omitted for clarity.

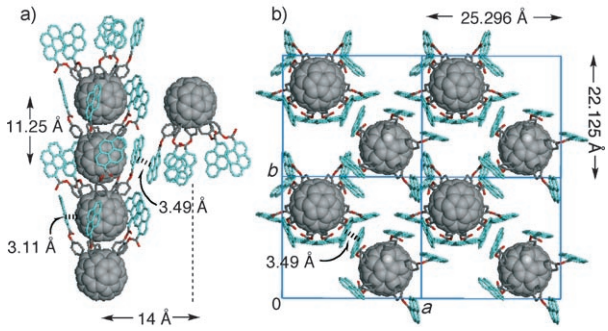

Figure 8. Crystal packing of **3**. a) A side view. b) A top view. A single layer is shown in this figure. The solvent molecules have been omitted for clarity. The crystal is monoclinic, space group $P2_1/c$ (No. 14), $a=22.125(5)$ Å, $b=25.296(5)$ Å, $c=22.351(5)$ Å, $\beta=90.49(5)°$, $V=12508.8(9)$ Å^3.

pyrene separation in **3** is 3.11 Å, which is 10% shorter than that in **1**. The interfullerene distance within the column for **3** is 11.25 Å, which is long, as a result of the presence of the cyclopentadiene hydrogen atom in the bottom of the cavity.

Energy-Transfer Properties and Supramolecular Interactions in Solution

The pyrene and fullerene groups have their own characteristic absorption and emission properties. The pyrene molecule itself shows a strong absorption in the UV region, with an absorption maximum at $\lambda^{abs}=336$ nm ($\varepsilon=4.8\times10^4\,M^{-1}cm^{-1}$). The fluorescence of the pyrene molecule $C_{16}H_{10}$ occurred through monomer and excimer emissions ($\lambda^{em}=360$–420 and 440–540 nm, respectively) with a large fluorescence quantum yield. The penta(organo)[60]fullerenes generally showed a broad UV absorption, featuring a characteristic absorption maximum at about 340–360 nm ($\varepsilon\approx2\times10^5\,M^{-1}cm^{-1}$) and weaker absorptions in the visible range extending to $\lambda^{abs}\approx670$ nm (Table 1). On the other hand, the penta(organo)[60]fullerenes showed a very weak fluorescence at $\lambda^{abs}\approx630$ nm (in toluene, for $C_{60}Me_5H$, $\phi=2.2\times10^{-3}$, and for $C_{60}Ph_5H$, $\phi=1.5\times10^{-3}$).[11]

Table 1. Spectroscopic data of **1**–**4** in a 5 μM solution at 25°C.

Compd	Solvent	λ_{max}^{abs} [nm] ([eV])	ε [$M^{-1}cm^{-1}$]	λ_{max}^{em} [nm] ([eV])	ϕ[a]
1	CH_2Cl_2	357 (3.47)	2.1×10^5	460 (2.70)	1.7×10^{-3}
1	toluene	357 (3.47)	2.1×10^5	450 (2.76)	n.d.
2	$CHCl_3$	347 (3.57)	2.0×10^5	437 (2.84)	1.1×10^{-2}
3	$CHCl_3$	357 (3.47)	1.7×10^5	420 (2.95), 441[b] (2.81)	1.2×10^{-2}
4	$CHCl_3$	345 (3.59)	2.2×10^5	395[b] (3.14), 483 (2.57)	3.3×10^{-3}
pyrene	cyclohexane	336 (3.36)	4.8×10^4	369 (3.36), 437 (2.62)[b]	0.65

[a] Quantum yield was determined using rhodamine B as a standard. [b] Shoulder peak. n.d. = not determined.

The UV absorption spectra of **1** to **4** are roughly superimpositions of those of the individual components, fullerene and pyrene, except that the pyrene absorption of **1** (357 nm) was more red shifted than the other compounds (Figure 9a), because of the strong intramolecular electronic interaction of the fullerene and the pyrene moieties in **1**. The most remarkable observation is the very low quantum yield of the emission of **1**–**4** (ϕ on the order of 10^{-3} to 10^{-2}), as opposed to the very high value of pyrene itself ($\phi=0.65$). The fluorescence quantum yield decreased to $\phi=1.7\times10^{-3}$ for **1** and 3.3×10^{-3} for **4**, compared to the strong emission of the pyrene groups.

Interestingly, the fluorescence spectra of **1** and **4** showed maxima at $\lambda^{em}=460$ nm and 483 nm, respectively, indicating that the emission occurred from a dimeric pyrene excimer even at very low concentrations of 5×10^{-6} M, accompanied by weak emission of the fullerene 50π-electron systems at $\lambda^{em}=620$–630 nm (Figure 9b). No, or very small, emission of the monomeric pyrene group was observed. Therefore, we conclude that the excimer emission occurred intramolecularly from neighboring pyrene groups. In **1**, the dimer responsible for the excimer emission is the one formed by the twisting of the propeller structure (Figures 5 and 10), and in **4**, the excimer emission is due to an intramolecular pyrene–pyrene interaction, as shown in Figure 10. Flexible spacers in **4** likely contribute to form the dimeric structure of the pyrene groups within the molecule.

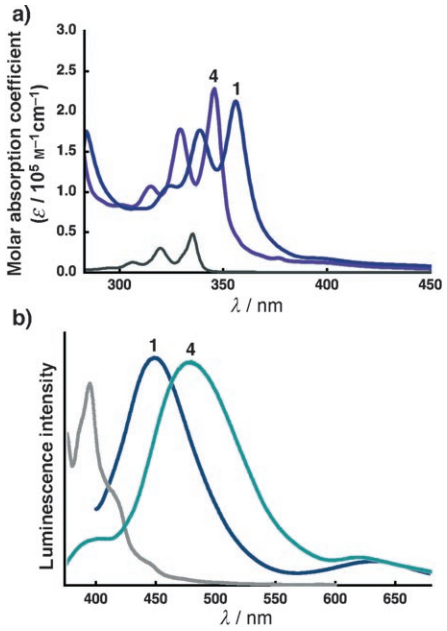

Figure 9. a) Absorption spectra of **1** (blue line), **4** (purple line), and pyrene (gray line). b) Emission spectra of **1** (blue line), **4** (green line), and pyrene (gray line). Solvents: cyclohexane (pyrene), toluene (**1**), and chloroform (**4**). Concentration: 1.0×10^{-5} M (absorption) and 1.0×10^{-6} M (emission).

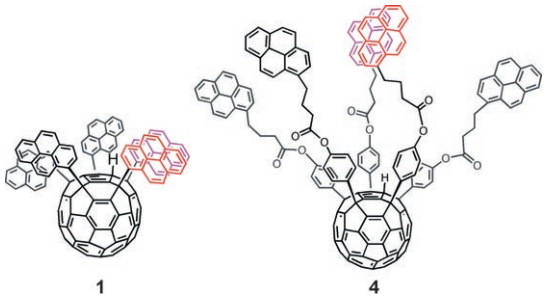

Figure 10. Intramolecular interaction between the neighboring pyrene groups of **1** and **4**.

In contrast, compounds **2** and **3** did not show any excimer emission (i.e., no emission at $\lambda^{em}=460$–480 nm), but showed weak monomer emission $\lambda^{em}=437$ nm and 420 nm, respectively, with quantum yields of $\phi=1.1\times10^{-2}$ and 1.2×10^{-2}, respectively. The tether connecting the pyrene and the fuller-

ene moieties was neither very short nor very long, and therefore, the pyrene moieties in a dilute solution could only emit light as the monomer.

Conclusions

In this study, we have reported on the efficient synthesis of fullerene–pyrene hybrid molecules, penta(pyrenyl)[60]fullerenes that bear five pyrene groups. The molecules form either a head-to-tail columnar array (for **3**) featuring fullerene–pyrene interactions, or a linear fullerene array featuring strong fullerene–fullerene interactions (for **1**). The photoenergy absorbed by the pyrene units was readily transferred to the fullerene moiety, and hence, the pyrene fluorescence was largely quenched. A low residual fluorescence was due to excimers in molecules of **1** and **4**, and due to monomers in **2** and **3**. This difference can be ascribed to either structural flexibility or to the inflexibility of the tether connecting the pyrene and the fullerene moieties. We recently reported that fullerene molecules related to those reported above can be attached to an indium tin oxide surface and allowed to generate photoelectric current with a quantum yield of about 20% (irradiation at 400 nm).[12] Therefore, we expect that installation of a light-harvesting antenna similar to the above pyrene rings would enhance the efficiency of such a molecular photovoltaic device.

Experimental Section

General

All the reactions dealing with air- or moisture-sensitive compounds were performed in an oven-dried reaction vessel under an argon or nitrogen atmosphere using standard Schlenk techniques. Air- and moisture-sensitive liquids and solutions were transferred via a syringe or a stainless steel cannula. Analytical thin-layer chromatography (TLC) was performed on glass plates with 0.25 mm 230–400 mesh silica gel containing a fluorescent indicator (Merck, #1.05715.0009). The TLC plates were visualized by exposure to an ultraviolet lamp (254 nm and/or 356 nm). Flash column chromatography was performed on Kanto Silica gel 60 (spherical, neutral, 140–325 mesh), as described by Still et al.[13] The water content of the solvents was determined to be less than 30 ppm using a Karl Fischer moisture titration (MK-210, Kyoto Electronics Co., Japan). High-performance liquid chromatography (HPLC) was used to monitor the reactions (column = Nomura Chemical Develosil RPFullerene, 4.6×250 mm or Nacalai Tesque Cosmosil Buckyprep, 4.6×250 mm, detector = Shimadzu SPD-M10Avp, detection at 350 nm). The fluorescence quantum yields were determined according to a literature procedure.[14] The yields were calculated based on the starting fullerene compounds.

All ^{1}H NMR spectra were taken at 500 MHz (JEOL ECA-500 spectrometer). The chemical shift values for the protons were reported in parts per million (ppm, δ scale) from an internal tetramethylsilane standard ($\delta = 0.00$ ppm) or from the residual protons of the deuterated solvent for ^{1}H NMR (e.g., $\delta = 7.26$ ppm for chloroform), and from the solvent carbon atoms (e.g., $\delta = 77.00$ ppm for chloroform) for the ^{13}C NMR data. The data were presented as follows: chemical shift, multiplicity (s = singlet, d = doublet, m = multiplet and/or multiplet resonances), coupling constant (in Hz), signal area integration in natural numbers, and assignment (in italics). The IR spectra were recorded using a React IR 1000 Reaction Analysis System equipped with DuraSample IR (ASI Applied System) and were reported in cm^{-1}. The UV/Vis and fluorescence spectra were recorded using Hitachi U3500 and Hitachi F4010 spectrometers, respectively. The mass spectra were recorded using Waters ZQ2000 or JEOL JMS T100 LC mass spectrometers.

Materials: All commercially available reagents, except those noted below, were used after nitrogen saturation or recrystallization. Anhydrous tetrahydrofuran (THF) was purchased from Kanto Chemical Co., Inc. (free from stabilizer) and dried by distillation over a Na/K alloy. The 1,2-$Cl_2C_6H_4$ used was dried by distillation from CaH_2 and stored under 4 Å molecular sieves. The CuBr·SMe_2 used was freshly prepared from CuBr (washed with methanol before use) and dimethyl sulfide and reprecipitated from pentane.[15] A solution of KO*t*Bu in THF was purchased from Aldrich Inc., and was used as received. The 1-pyreneboronic acid,[16] 1-(4-bromophenyl)pyrene,[17] and pyrene-1-carboxylic acid[18] were prepared according to a literature procedure. The penta(4-hydroxyphenyl)[60]fullerene, $C_{60}(C_6H_4OH)_5H$, was synthesized according to a previous report.[7a]

Synthesis

1: A THF solution of 1-pyrenylmagnesium bromide (0.70 M, 10 mL, 7.0 mmol) at 0 °C was added to a suspension of CuBr·SMe_2 (1.44 mg, 7.0 mmol) and C_{60} (500 mg, 0.70 mmol) in 1,2-$Cl_2C_6H_4$ (20 mL). The reaction mixture was then warmed to 25 °C, and stirred for a period of 12 h. The reaction was monitored using HPLC (Buckyprep, eluent = 7:3 toluene/2-propanol, flow rate = 2.0 mL min^{-1}, retention time = 5.1 min), until completion of the reaction. The reaction was quenched by using an aqueous saturated NH_4Cl solution (ca. 0.5 mL), followed by the removal of any volatile materials under reduced pressure. The mixture was diluted with toluene and CS_2 (5:5 toluene/CS_2, ca. 200 mL) and filtered through a pad of silica gel. The orange-colored eluent was evaporated to obtain a solid. The crude product was purified using silica gel column chromatography (0%–5% toluene in CS_2) to obtain the desired compound (880 mg, 70%) as a red solid after recrystallization using CS_2 and ethanol. ^{1}H NMR (500 MHz, $CDCl_3$): $\delta = 5.30$ (d, $J = 9.5$ Hz, 1H, $C_{16}H_9$), 6.26 (s, 1H, C_{60}-*H*), 6.86 (d, $J = 7.7$ Hz, 1H, $C_{16}H_9$), 6.94 (d, $J = 8.3$ Hz, 1H, $C_{16}H_9$), 7.24 (d, $J = 9.7$ Hz, 2H, $C_{16}H_9$), 7.50 (d, $J = 8.3$ Hz, 2H, $C_{16}H_9$), 7.56–7.64 (m, 7H, $C_{16}H_9$), 7.70 (t, $J = 8.5$ Hz, 2H, $C_{16}H_9$), 7.76 (d, $J = 8.8$ Hz, 1H, $C_{16}H_9$), 7.79 (d, $J = 8.8$ Hz, 2H, $C_{16}H_9$), 7.82 (d, $J = 8.8$ Hz, 1H, $C_{16}H_9$), 7.89 (d, $J = 8.5$ Hz, 2H, $C_{16}H_9$), 7.91 (d, $J = 7.2$ Hz, 2H, $C_{16}H_9$), 7.95–7.99 (m, 8H, $C_{16}H_9$), 8.03 (d, $J = 9.1$ Hz, 2H, $C_{16}H_9$), 8.07 (d, $J = 7.5$ Hz, 1H, $C_{16}H_9$), 8.19 (d, $J = 7.1$ Hz, 2H, $C_{16}H_9$), 8.78 (t, $J = 8.0$ Hz, 4H, $C_{16}H_9$), 8.81 (d, $J = 9.8$ Hz, 2H, $C_{16}H_9$), 9.87 ppm (d, $J = 9.5$ Hz, 2H, $C_{16}H_9$); IR (ReactIR diamond probe): $\tilde{\nu} = 3043$, 2964, 2930, 1507, 1496, 1459, 1436, 1415, 1291, 1248, 1214, 1181, 1166, 1142, 1111, 971, and 967 cm^{-1}; APCI-HRMS (−) calcd for $C_{140}H_{45}$ $[M-H]^-$: 1725.3521; found: 1725.3523.

1′: All the methylated compounds **1′**–**4′** were synthesized using a deprotonation/methylation method according to a previous report.[8] A THF solution of 1-pyrenylmagnesium bromide (0.70 M, 10 mL, 7.0 mmol) was added to a suspension of CuBr·SMe_2 (1.4 g, 7.0 mmol) and C_{60} (500 mg, 0.70 mmol) in 1,2-$Cl_2C_6H_4$ (20 mL) at 0 °C. The reaction mixture was stirred at 25 °C for a period of 12 h. The reaction was monitored using HPLC to confirm the conversion of the reaction. Methyl iodide (0.44 mL) was added to this solution, and then the reaction solution was refluxed. HPLC analysis suggested the completion of the methylation after a period of 6 h (Buckyprep, eluent = 7:3 toluene/2-propanol, flow rate = 2.0 mL min^{-1}, retention time = 4.9 min). After the removal of any volatile materials under reduced pressure, the crude mixture was diluted with toluene and CS_2 (5:5 toluene/CS_2, ca. 200 mL) and filtered through a pad of silica gel. The orange-colored eluent was evaporated to obtain a solid. The crude product was purified using silica gel column chromatography (0%–5% toluene in CS_2) to obtain the desired compound (920 mg, 73%) as a red solid after recrystallization with CS_2 and ethanol. ^{1}H NMR (500 MHz, $CDCl_3$): $\delta = 1.97$ (s, 3H, C_{60}-CH_3), 5.18 (d, $J = 9.1$ Hz, 1H, $C_{16}H_9$), 6.66 (d, $J = 7.5$ Hz, 1H, $C_{16}H_9$), 6.92 (d, $J = 8.0$ Hz, 1H, $C_{16}H_9$), 7.10 (d, $J = 9.1$ Hz, 1H, $C_{16}H_9$), 7.17 (d, $J = 9.1$ Hz, 1H, $C_{16}H_9$), 7.38–7.47 (m, 2H, $C_{16}H_9$), 7.53 (d, $J = 8.5$ Hz, 1H, $C_{16}H_9$), 7.59–7.65 (m, 5H, $C_{16}H_9$), 7.69 (d, $J = 9.1$ Hz, 1H, $C_{16}H_9$), 7.69–7.89 (m, 8H, $C_{16}H_9$), 7.95–8.12 (m,

10H, $C_{16}H_9$), 8.17–8.25 (m, 6H, $C_{16}H_9$), 8.69 (d, J=9.1 Hz, 1H, $C_{16}H_9$), 8.78 (d, J=10.1 Hz, 1H, $C_{16}H_9$), 8.85 (d, J=8.0 Hz, 1H, $C_{16}H_9$), 8.91 (d, J=8.0 Hz, 1H, $C_{16}H_9$), 9.03 (d, J=8.0 Hz, 1H, $C_{16}H_9$), 9.06 (d, J=8.0 Hz, 1H, $C_{16}H_9$), 9.36 (d, J=9.5 Hz, 1H, $C_{16}H_9$), 9.41 (d, J=10.0 Hz, 1H, $C_{16}H_9$), 9.98 (d, J=9.1 Hz, 1H, $C_{16}H_9$), 10.10 ppm (d, J=9.5 Hz, 1H, $C_{16}H_9$); ^{13}C NMR (125 MHz, $CDCl_3$): δ=26.53 (C_{60}-CH_3), 60.34, 63.55, 64.48, 64.54, 64.96, 70.63, 123.85–131.35 ($C_{16}H_9$), 135.13, 139.15, 141.22, 141.37, 141.79, 143.72, 143.86, 143.88, 143.90, 144.04, 144.16, 144.17, 144.23, 144.28, 144.85, 144.89, 145.43, 145.56, 145.93, 146.17, 146.55, 147.63, 147.86, 147.97, 148.08, 148.15, 148.18, 148.29, 148.33, 148.56, 148.68, 148.74, 148.76, 148.85, 149.02, 149.15, 149.19, 149.72, 151.35, 153.83, 155.67, 155.93, 158.36, 159.58, 160.45, 162.07, 162.43, 165.58 ppm; IR (ReactIR diamond probe): $\tilde{\nu}$=3043, 2964, 2930, 1507, 1496, 1459, 1436, 1415, 1291, 1248, 1214, 1181, 1166, 1142, 1111, 971, and 967 cm^{-1}; APCI-MS (−): m/z: 1739 ([M]$^-$).

2: A solution of C_{60} (50 mg, 0.070 mmol) in 1,2-$Cl_2C_6H_4$ (2.0 mL) was added at 0°C to an organocopper reagent prepared from 4-(1-pyrenyl)C_6H_4MgBr[19](0.60 M, 1.2 mL, 0.70 mmol) and CuBr·SMe_2 (140 mg, 0.70 mmol) in THF (1.0 mL). The resulting dark brown suspension was gradually warmed to 25°C over a period of 30 min. The reaction was monitored using HPLC, suggesting the reaction was complete after 6 h (Buckyprep, eluent=7:3 toluene/2-propanol). The reaction was quenched with an aqueous saturated NH_4Cl solution (ca. 0.05 mL), followed by the removal of any volatile materials under reduced pressure. The mixture was diluted with toluene and CS_2 (5:5 toluene/CS_2, ca. 20 mL) and filtered through a pad of silica gel. After an orange-colored eluent was evaporated to obtain a solid, the crude product was purified using silica gel column chromatography (0%–5% toluene in CS_2) to obtain the desired compound (110 mg, 72%) as an orange solid. ^{1}H NMR (500 MHz, $CDCl_3$): δ=5.74 (s, 1H, C_{60}-H), 7.37–7.40 (m, 8H, C_6H_4), 7.47, 7.49 (m, 4H, C_6H_4), 7.57–7.60 (m, 8H, C_6H_4), 7.67–7.76, 7.78–7.84, 7.85, 7.87, 7.88–7.90, 7.92, 7.94, 7.95, 7.96, 7.97–7.98, 7.99–8.20, 8.18–8.20, 8.23, 8.25 ppm (m, 45H, $C_{16}H_9$); ^{13}C NMR (125 MHz, $CDCl_3$): δ=34.75, 58.03, 58.97, 61.02, 124.57–125.24, 125.88–126.02, 127.06–128.45, 130.52–131.47, 136.64, 136.77, 137.12, 138.66, 139.43, 139.67, 140.24, 140.67, 140.83, 143.97, 144.22, 144.35, 144.33, 144.57, 144.63, 144.77, 145.84, 146.08, 147.14, 147.22, 147.87, 148.24, 148.57, 148.71, 148.80, 148.97, 152.34, 152.67 ppm; IR (ReactIR diamond probe); $\tilde{\nu}$=3037, 2964, 2933, 2848, 1602, 1584, 1559, 1517, 1497, 1488, 1459, 1434, 1418, 1405, 1289, 1192, 1177, 1111, 1073, 1023, 1005, and 967 cm^{-1}; APCI-MS (−): m/z: 2105 ([M]$^-$).

Preparation of acid chlorides: Pyrene-1-carbonyl chloride: To a mixture of pyrene-1-carboxylic acid (5.0 g, 2.05 mmol) and DMF (60 μL, 0.72 mmol) in dichloromethane (100 mL), thionyl chloride (0.4 mL, 5.2 mmol) was added dropwise at a rate sufficient to maintain a steady evolution of gas. This solution was heated at reflux for a period of 2 h and cooled to ambient temperature, and the excess thionyl chloride was removed in vacuo to give the acid chloride, which was used in the next reaction without further purification. 4-(Pyren-1-yl)butanoyl chloride was prepared using the same procedure.

3: To a mixture of $C_{60}(C_6H_4OH)_5H$ (200 mg, 0.17 mmol) and pyrene-1-carbonyl chloride (300 mg, 1.1 mmol) in THF (80 mL), triethylamine (0.16 mL, 1.2 mmol), and 4-dimethylaminopyridine (140 mg, 1.2 mmol) were added at 0°C. The reaction was monitored using HPLC, suggesting the reaction was complete after a period of 3 h (RPFullerene, eluent=5:5 toluene/methanol, flow rate=2.0 mL min^{-1}, retention time=5.0 min). After the solvent was removed under reduced pressure, the resulting crude product was purified using silica gel column chromatography with CS_2 and chloroform (5:5 CS_2/chloroform) as eluents, and recrystallized using chloroform and ethanol to obtain the desired compound (280 mg, 70%) as reddish-orange microcrystals. ^{1}H NMR (500 MHz, $CDCl_3$): δ=5.56 (s, 1H, C_{60}-H), 7.36–7.41 (m, 8H, C_6H_4), 7.47–7.51 (m, 4H, C_6H_4), 7.65–7.68 (m, 8H, C_6H_4), 7.83–8.36, 8.87–8.93, 9.29, 9.30, 9.34–9.37, 9.51, 9.53 ppm (m, 45H, $C_{16}H_9$). ^{13}C NMR (125 MHz, $CDCl_3$): δ=58.4, 58.6, 62.1, 63.1, 93.8, 99.7, 121.0, 121.7, 121.8, 122.5–122.8, 123.8–124.0, 124.7–125.0, 126.0–126.4, 126.5, 126.8–127.1, 128.8, 129.0–129.3, 129.7–130.2, 130.5–130.8, 131.8–131.9, 132.6, 134.6, 134.7, 135.5, 136.8, 136.9, 141.3, 142.8, 142.9, 143.3, 143.6, 143.9, 144.2, 144.2–144.8, 145.2, 145.4, 145.7, 145.8, 146.8, 147.0, 147.1, 147.7, 148.0, 148.1, 148.2, 148.4, 148.6–148.8, 150.2, 150.7, 150.9, 151.3, 151.5, 151.9, 152.3, 155.0, 156.0, 159.163.1, 165.4 ppm; IR (ReactIR diamond probe): $\tilde{\nu}$=3043, 2964, 2952, 2890, 1727 (s), 1596 (s), 1503 (s), 1385, 1328, 1248, 1229, 1206, 1191, 1142, 1123, 1123, 1079, 1017, 1017, and 971 cm^{-1}; APCI-MS (−): m/z: 2325 ([M]$^-$).

4: Compound **4** was synthesized using the same synthetic route as **3** starting from $C_{60}(C_6H_4OH)_5H$ (300 mg, 0.25 mmol) and 4-(pyren-1-yl)butanoyl chloride (520 mg, 1.7 mmol). The desired compound was obtained as an orange solid (560 mg, 87%). ^{1}H NMR (500 MHz, $CDCl_3$). δ=2.07–2.18 (m, 10H, CH_2), 2.44–2.52 (m, 10H, CH_2), 3.17–3.26 (m, 10H, CH_2), 5.18 (s, 1H, C_{60}-H), 6.88–6.92 (m, 10H, C_6H_4), 6.99–7.01 (m, 10H, C_6H_4), 7.31, 7.33, 7.49, 7.50, 7.61–8.13, 8.19, 8.21, 8.23, 8.25, 8.28, 8.29, 8.31 ppm (m, 45H, $C_{16}H_9$); ^{13}C NMR (125 MHz, $CDCl_3$): δ=26.54, 26.83, 32.46, 32.54, 33.77, 33.93, 63.17, 93.84, 99.71, 122.08, 122.16, 123.13, 123.23, 124.77, 124.85, 124.91, 125.35, 125.73, 126.67, 127.24, 127.36, 127.42, 128.27, 128.34–129.07, 129.83, 130.78, 130.92, 131.45, 131.57, 135.32–136.16, 136.93, 137.07, 137.82, 142.87, 143.04, 143.27, 143.93, 144.07, 144.12, 144.25, 144.97, 145.22, 145.57, 146.81, 146.94, 147.02, 147.27, 147.53, 147.98, 148.04, 148.18, 148.24, 148.58, 148.62, 149.19–150.14, 151.12, 151.75, 152.33, 155.67, 171.64, 171.77, 173.42 ppm; IR (ReactIR diamond probe): $\tilde{\nu}$=3041, 2939, 2875, 1756 (s), 1603 (w), 1503 (s), 1459, 1416, 1208, 1169, 1123 (s), 1017, 1017, and 841 cm^{-1}; APCI-MS (−): m/z: 2535 ([M]$^-$).

X-ray Crystallographic Analysis

The data sets of **1** and **3** were collected using a MacScience DIP2030 Imaging Plate diffractometer employing $Mo_{K\alpha}$ radiation (graphite monochromated, λ=0.71069 Å). The positional and thermal parameters of the non-hydrogen atoms were refined anisotropically on F^2 using the full-matrix least-squares method employing the SHELXL-97 software program.[20] The hydrogen atoms were placed at the calculated positions and refined using a riding mode on their corresponding carbon atoms. CCDC-682300 and 682301 contain the supplementary crystallographic data for this paper.

Electrochemical Measurements

Cyclic voltammetry and differential pulse voltammetry were performed using a Hokuto Denko HZ-5000 voltammetric analyzer. A glassy carbon electrode, platinum coil, and an Ag/Ag^+ electrode were used as the working, counter, and reference electrodes, respectively. All half-wave potentials $E_{1/2}=(E_{pc}+E_{pa})/2$, where E_{pc} and E_{pa} are the cathodic and anodic peak potentials, respectively, were corrected against a ferrocene/ferrocenium couple, Fc/Fc^+.

Theoretical Calculations

All the theoretical calculations were performed using the Gaussian 03 software package. The density functional theory (DFT) method was employed using the B3LYP hybrid functional.[21] A 6-31G* basis set was used for the geometry optimization of model compounds **1** and **1′**.[22]

Acknowledgements

This study was partially supported by the 21st century COE Program for Frontiers in Fundamental Chemistry and the Global COE Program for Chemistry Innovation from the Ministry of Education, Culture, Sports, Science and Technology, Japan.

[1] For the fullerene–pyrene hybrids: a) Y. Nakamura, T. Minowa, S. Tobita, H. Shizuka, J. Nishimura, *J. Chem. Soc. Perkin Trans. 2* **1995**, 2351–2357; b) T. Gareis, O. Köthe, J. Daub, *Eur. J. Org. Chem.* **1998**, 1549–1557; c) R. B. Martin, K. Fu, Y.-P. Sun, *Chem. Phys. Lett.* **2003**, *375*, 619–624; d) F. Hauke, S. Atalick, D. M. Guldi, J. Mack, L. T. Scott, A. Hirsch, *Chem. Commun.* **2004**, 766–767; e) A. D. Darwish, A. G. Avent, A. K. Abdul-Sada, I. V. Gol′dt, P. B. Hitchcock, I. V. Kuvytchko, R. Taylor, *Chem. Eur. J.* **2004**, *10*, 4523–

4531; f) F. Hauke, A. Hirsch, S. Atalick, D. M. Guldi, *Eur. J. Org. Chem.* **2005**, 1741–1751.

[2] a) M. I. Sluch, I. D. W. Samuel, M. C. Petty, *Chem. Phys. Lett.* **1997**, *280*, 315–320; b) F. Perret, M. Nishihara, T. Takeuchi, S. Futaki, A. N. Lazar, A. W. Coleman, N. Sakai, S. Matile, *J. Am. Chem. Soc.* **2005**, *127*, 1114–1115; c) M. Nishihara, F. Perret, T. Takeuchi, S. Futaki, A. N. Lazar, A. W. Coleman, N. Sakai, S. Matile, *Org. Biomol. Chem.* **2005**, *3*, 1659–1669.

[3] a) G. McDermott, S. M. Prince, A. A. Freer, A. M. Hawthornthwaite-Lawless, M. Z. Papiz, R. J. Cogdell, N. W. Issacs, *Nature* **1995**, *374*, 517–521; b) W. Kuhlbrandt, *Nature* **1995**, *374*, 497–498.

[4] a) M. Helmreich, E. A. Ermilov, M. Meyer, N. Jux, A. Hirsch, B. Röder, *J. Am. Chem. Soc.* **2005**, *127*, 8376–8385; b) D. M. Guldi, M. Marcaccio, F. Paolucci, D. Paolucci, J. Ramey, R. Taylor, G. A. Burley, *J. Phys. Chem. A* **2005**, *109*, 9723–9730; c) H. Li, A. Kitaygorodskiy, R. A. Carino, Y.-P. Sun, *Org. Lett.* **2005**, *7*, 859–861.

[5] a) S. Xiao, Y. Li, Y. Li, J. Zhuang, N. Wang, H. Liu, B. Ning, Y. Liu, F. Lu, L. Fan, C. Yang, Y. Li, D. Zhu, *J. Phys. Chem. B* **2004**, *108*, 16677–16685; b) S. Xiao, M. E. El-Khouly, Y. Li, Z. Gan, H. Liu, L. Jiang, Y. Araki, O. Ito, D. Zhu, *J. Phys. Chem. B* **2005**, *109*, 3658–3667.

[6] a) M. Sawamura, H. Iikura, E. Nakamura, *J. Am. Chem. Soc.* **1996**, *118*, 12850–12851; b) Y. Matsuo, A. Muramatsu, K. Tahara, M. Koide, E. Nakamura, *Org. Synth.* **2006**, *83*, 80–87.

[7] a) M. Sawamura, K. Kawai, Y. Matsuo, K. Kanie, T. Kato, E. Nakamura, *Nature* **2002**, *419*, 702–705; b) Y. Matsuo, A. Muramatsu, Y. Kamikawa, T. Kato, E. Nakamura, *J. Am. Chem. Soc.* **2006**, *128*, 9586–9587.

[8] R. Hamasaki, Y. Matsuo, E. Nakamura, *Chem. Lett.* **2004**, *33*, 328–329.

[9] H. Iikura, S. Mori, M. Sawamura, E. Nakamura, *J. Org. Chem.* **1997**, *62*, 7912–7913.

[10] Y. Matsuo, A. Muramatsu, R. Hamasaki, N. Mizoshita, T. Kato, E. Nakamura, *J. Am. Chem. Soc.* **2004**, *126*, 432–433.

[11] a) D. M. Guldi, G. M. A. Rahman, R. Marczak, Y. Matsuo, M. Yamanaka, E. Nakamura, *J. Am. Chem. Soc.* **2006**, *128*, 9420–9427; b) Y. Matsuo, K. Matsuo, T. Nanao, R. Marczak, S. S. Gayathri, D. M. Guldi, E. Nakamura, *Chem. Asian J.* **2008**, *3*, 841–848.

[12] Y. Matsuo, K. Kanaizuka, K. Matsuo, Y.-W. Zhong, T. Nakae, E. Nakamura, *J. Am. Chem. Soc.* **2008**, *130*, 5016–5017.

[13] W. C. Still, M. Kiahn, A. Mitra, *J. Org. Chem.* **1978**, *43*, 2923–2924.

[14] J. N. Demas, G. A. Crosby, *J. Phys. Chem.* **1971**, *75*, 991–1024.

[15] A. B. Theis, C. A. Townsend, *Synth. Commun.* **1981**, *11*, 157–166.

[16] N. Amann, E. Pandurski, T. Fiebig, H.-A. Wagenknecht, *Angew. Chem.* **2002**, *114*, 3084–3087; *Angew. Chem. Int. Ed.* **2002**, *41*, 2978–2980.

[17] J. Daub, R. Engl, J. Kurzawa, S. E. Miller, S. Schneider, A. Stockmann, M. R. Wasielewski, *J. Phys. Chem. A* **2001**, *105*, 5655–5665.

[18] M. Barfield, M. J. Collins, J. E. Gready, S. Sternhell, C. W. Tansey, *J. Am. Chem. Soc.* **1989**, *111*, 4285–4290.

[19] A Grignard reagent, 4-(1-pyrene)phenylmagnesium bromide was prepared using a standard method employing 1-(4-bromophenyl)pyrene in a mixed solvent of THF and toluene (2:1).

[20] G. M. Sheldrick, *Programs for Crystal Structure Analysis*, Institut für Anorganische Chemie der Universität Göttingen, Germany, **1998**.

[21] a) A. D. Becke, *J. Chem. Phys.* **1993**, *98*, 5648–5652; b) C. Lee, W. Yang, R. G. Parr, *Phys. Rev. B* **1988**, *37*, 785–789.

[22] W. J. Hehre, L. Radom, P. von R. Schleyer, J. A. Pople, *Ab Initio Molecular Orbital Theory*, Wiley, New York, **1986**.

Received: March 25, 2008
Published online: July 21, 2008

